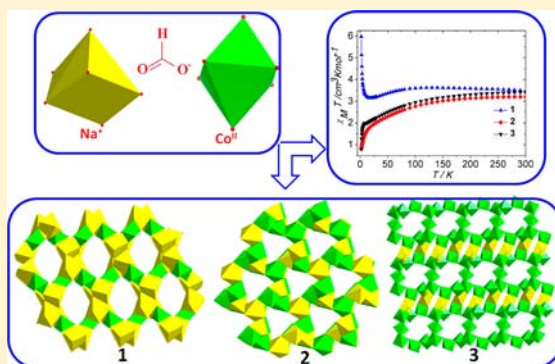


## Tuning the Structure and Magnetism of Heterometallic Sodium(1+)–Cobalt(2+) Formate Coordination Polymers by Varying the Metal Ratio and Solvents

Jiong-Peng Zhao,<sup>†,‡</sup> Song-De Han,<sup>†</sup> Ran Zhao,<sup>†</sup> Qian Yang,<sup>†</sup> Ze Chang,<sup>†</sup> and Xian-He Bu<sup>\*,†</sup><sup>†</sup>Department of Chemistry and TKL of Metal and Molecule-based Material Chemistry, Nankai University, Tianjin 300071, China<sup>‡</sup>School of Chemistry and Chemical Engineering, Tianjin University of Technology, Tianjin 300384, China

## S Supporting Information

**ABSTRACT:** Three new heterometallic formate coordination polymers formulated as  $[\text{Na}_2\text{Co}(\text{HCOO})_4]_\infty$  (**1**),  $[\text{NaCo}(\text{HCOO})_3]_\infty$  (**2**), and  $[\text{Na}_2\text{Co}_7(\text{HCOO})_{16}]_\infty$  (**3**) were obtained by adjusting the solvent and ratio of the reactants. In **1**, a (4,4) cobalt formate layer is formed and the sodium ions connect the layers to form a three-dimensional (3D) framework. In **2**, each formate ligand binds two  $\text{Co}^{2+}$  and two  $\text{Na}^+$  ions with a syn,syn,anti,anti coordination mode to form a chiral network with 4,6-connected topology. **3** is a  $\text{Na}^+$ -ion-linked 3D framework based on the cobalt formate layer, which has a 10-membered metal ring. Magnetic studies indicate the existence of ferromagnetic interactions between adjacent  $\text{Co}^{2+}$  ions in **1**, while dominating antiferromagnetic couplings in **2** and **3**.



## INTRODUCTION

In recent years, the investigation of coordination polymer-based magnets and the magnetostructural relationship had become the focus of intense researches for their unusual structures and physical properties.<sup>1</sup> Although significant progress has been made in practical and theoretical approaches, the design and synthesis of coordination polymers with desirable magnetic properties is still a tremendous challenge. The key point in constructing new molecule-based magnets with desired structures and properties is how to judiciously choose the appropriate bridging ligands, which can help to realize the fine-tuning of the local interactions between spin carriers and form the targeted product via self-assembly between paramagnetic metal centers and ligands.<sup>2</sup> A good candidate as a short bridging ligand that could mediate magnetic coupling effectively, a formate anion with diverse binding ability is used extensively to construct molecule magnetic materials.<sup>3</sup> Over the last decades, a huge number of formate metal complexes with diverse bridging modes such as  $\mu_2\text{-O}/\text{syn,syn}/\text{anti,anti}/\text{syn,syn}/\text{anti,syn}/\text{anti,anti}$  and  $\text{syn,syn}/\text{anti,anti}$  modes of formate and various types of structures from a zero-dimensional cluster to one-dimensional (1D) chains, two-dimensional (2D) layers, and three-dimensional (3D) networks have been reported.<sup>4,5</sup> A variety of magnetic phenomena, such as ferromagnetic behavior, antiferromagnetic ordering, spin canting, etc., have also been observed in such complexes.<sup>6</sup>

Among various metal formates, cobalt-based complexes are attractive because of their large single-ion anisotropy (good candidate for single-molecule and single-chain magnets) and the flexibility of the cobalt ion in adopting different

coordination modes, in terms of both the coordination number and geometry.<sup>7</sup> Furthermore, the magnetic behaviors could be more diverse in cobalt-involved heterometallic systems. In most of the reported heterometallic systems, the metal ions were paramagnetic 3d–3d or 3d–4f heterometal.<sup>8</sup> Little attention has been paid to introduce diamagnetic alkali-metal ions in such systems.<sup>9,10</sup> The introduction of alkali-metal ions may provide more variability to construct magnetic complexes with complicated structures, fantastic topologies, and particular coordination geometries, which may lead to unpredictable and interesting magnetic phenomena.

Herein, we report the synthesis and structures of three new heterometallic formate complexes with different Co/Na ratios formulated as  $[\text{Na}_2\text{Co}(\text{HCOO})_4]_\infty$  (**1**),  $[\text{NaCo}(\text{HCOO})_3]_\infty$  (**2**), and  $[\text{Na}_2\text{Co}_7(\text{HCOO})_{16}]_\infty$  (**3**). The structures of these complexes were found to be affected by the used solvents and Co/Na ratios of the reactants. Magnetic measurements revealed that the interaction between adjacent  $\text{Co}^{2+}$  ions in **1** was ferromagnetic, while dominating antiferromagnetic couplings were found in **2** and **3**. Furthermore, **3** was an antiferromagnet showing a spin-flop transition with critical field at ca. 4000 Oe.

## EXPERIMENTAL SECTION

**Materials and Physical Measurements.** All of the chemicals used for the synthesis were of analytical grade and were commercially available.

Received: September 4, 2012

Published: March 5, 2013

Elemental analyses (carbon, hydrogen, and nitrogen) were performed on a Perkin-Elmer 240C analyzer. The powder X-ray diffraction (PXRD) was recorded on a Rigaku D/Max-2500 diffractometer at 40 kV and 100 mA for a copper-target tube and a graphite monochromator. IR spectra were measured on a Tensor 27 OPUS (Bruker) Fourier transform IR spectrometer with KBr pellets. Thermogravimetric analysis (TGA) was carried out on a standard TGA-DTA analyzer under a nitrogen flow at a heating rate of 2 °C min<sup>-1</sup> for all measurements. Simulation of the PXRD spectra was done by the single-crystal data and diffraction-crystal module of the *Mercury* program available free of charge via the Internet at <http://www.iucr.org>.

Magnetic data were collected using well-crushed crystals of the samples on a Quantum Design MPMS-XL SQUID magnetometer equipped with a 7 T magnet. The data were corrected using Pascal's constants to calculate the diamagnetic susceptibility, and an experimental correction for the sample holder was applied.

**Synthesis of 1.** A mixture of Co(NO<sub>3</sub>)<sub>2</sub>·6H<sub>2</sub>O (1 mmol), NaHCOO (3 mmol), and *N,N*-dimethylformamide (DMF; 10 mL) was sealed in a Teflon-lined autoclave and heated to 140 °C. After being maintained for 48 h, the reaction vessel was cooled to room temperature in 12 h, and pure primrose-black crystals were collected with ca. 20–25% yield based on Co(NO<sub>3</sub>)<sub>2</sub>·6H<sub>2</sub>O. Anal. Calcd for C<sub>4</sub>H<sub>4</sub>CoNa<sub>2</sub>O<sub>8</sub> (1): C, 16.86; H, 1.41. Found: C, 16.95; H, 1.72.

**Synthesis of 2.** A mixture of Co(NO<sub>3</sub>)<sub>2</sub>·6H<sub>2</sub>O (1 mmol), NaHCOO (1 mmol), and DMF (10 mL) was sealed in a Teflon-lined autoclave and heated to 140 °C. After being maintained for 48 h, the reaction vessel was cooled to room temperature in 12 h, and pure primrose-black crystals were collected with ca. 20–25% yield based on Co(NO<sub>3</sub>)<sub>2</sub>·6H<sub>2</sub>O. Anal. Calcd for C<sub>3</sub>H<sub>3</sub>CoNaO<sub>6</sub> (2): C, 16.61; H, 1.39. Found: C, 16.38; H, 1.12.

**Synthesis of 3.** Method A: A mixture of Co(NO<sub>3</sub>)<sub>2</sub>·6H<sub>2</sub>O (1.5 mmol), NaHCOO (2 mmol), 2,6-pyridinedicarboxylic acid (H<sub>2</sub>L; 1.5 mmol), and DMF:MeOH = 1:1 (10 mL) was sealed in a Teflon-lined autoclave and heated to 140 °C. After being maintained for 48 h, the reaction vessel was cooled to room temperature in 12 h, and pure primrose-pink crystals were collected with ca. 20–25% yield based on Co(NO<sub>3</sub>)<sub>2</sub>·6H<sub>2</sub>O with complex Na<sub>2</sub>CoL<sub>2</sub> as commensalism.<sup>11</sup> Method B: Similar to method A, Co(NO<sub>3</sub>)<sub>2</sub>·6H<sub>2</sub>O (1.5 mmol), NaHCOO (0.4 mmol), NH<sub>4</sub>HCOO (2.4 mmol), and MeOH (10 mL) were used as reactants, and the yield is ca. 30–35% based on Co(NO<sub>3</sub>)<sub>2</sub>·6H<sub>2</sub>O. Anal. Calcd for C<sub>16</sub>H<sub>16</sub>Co<sub>7</sub>Na<sub>2</sub>O<sub>32</sub> (3): C, 16.30; H, 1.37. Found: C, 16.62; H, 1.65.

It is worth noting that the solvent and the ratio of the formate anion with Na<sup>+</sup> and Co<sup>2+</sup> ions are vital to obtaining the three complexes. Reacting sodium formate and Co<sup>2+</sup> using DMF as the solvent with a Co<sup>2+</sup>/Na<sup>+</sup> ratio of 1:2 yielded 1, while changing the Co<sup>2+</sup>/Na<sup>+</sup> ratio to 1:1 yielded 2. However, using mixed solvents (DMF:MeOH = 1:1) or MeOH as solvents and adjusting Co<sup>2+</sup>/Na<sup>+</sup> ratio of 7:2, 3 was obtained (3 could be synthesized in two different methods as mentioned above). The IR spectra for the three complexes are given in Figure S1 in the Supporting Information (SI), in which the absorption band ~2900 cm<sup>-1</sup> belongs to a C–H stretching vibration and the bands ~1600, ~1300–1400, and ~800 cm<sup>-1</sup> belong to O–C–O stretching and deformation vibrations. TGA results (Figure S2 in the SI) indicate that these complexes are stable until about 250 °C.

**X-ray Data Collection and Structure Determination.** Single-crystal X-ray diffraction data for 1–3 were collected on a Rigaku SCXmini diffractometer at 293(2) K with Mo K $\alpha$  radiation ( $\lambda$  = 0.71073 Å) by  $\omega$ -scan mode. The program Rigaku *CrystalClear*<sup>12a</sup> was used for integration of the diffraction profiles. All of the structures were solved by direct methods using the *SHELXS* program of the *SHELXTL* package and refined by full-matrix least-squares methods with *SHELXL* (semiempirical absorption corrections were applied using the *SADABS* program).<sup>12b</sup> Metal atoms in each complex were located from the *E* maps, and other non-hydrogen atoms were located in successive difference Fourier syntheses and refined with anisotropic thermal parameters on *F*<sup>2</sup>. The hydrogen atoms of the ligands were generated theoretically onto the specific atoms and refined isotropically with fixed thermal factors. Table 1 shows the crystallographic data

and structure-processing parameters. Selected bond lengths and angles are listed in Table 2.

**Table 1. Crystal Data and Structure Refinements for 1–3**

	1	2	3
chemical formula	C <sub>4</sub> H <sub>4</sub> CoNa <sub>2</sub> O <sub>8</sub>	C <sub>3</sub> H <sub>3</sub> CoNaO <sub>6</sub>	C <sub>16</sub> H <sub>16</sub> Co <sub>7</sub> Na <sub>2</sub> O <sub>32</sub>
fw	284.98	216.97	1178.78
space group	C2/c	I2 <sub>1</sub> 3	P $\bar{1}$
<i>a</i> /Å	15.694(3)	9.0327 (10)	8.2693(17)
<i>b</i> /Å	8.8836(18)	9.0327 (10)	8.4170(17)
<i>c</i> /Å	6.7448(13)	9.0327 (10)	12.645(3)
$\alpha$ /deg	90	90	90.27(3)
$\beta$ /deg	107.35(3)	90	95.85(3)
$\gamma$ /deg	90	90	100.93(3)
<i>V</i> /Å <sup>3</sup>	897.6(3)	736.97 (14)	859.4(3)
<i>Z</i>	4	4	4
GOF	1.202	1.21	1.151
<i>D</i> /g cm <sup>-3</sup>	2.109	1.956	2.278
$\mu$ /mm <sup>-1</sup>	2.028	2.37	3.437
<i>T</i> /K	293	293	293
<i>R</i> <sup>a</sup> / <i>R</i> <sub>w</sub> <sup>b</sup>	0.0252/0.0609	0.0133/0.0356	0.0842/0.1464
$\alpha R = \sum   F_o  -  F_c   / \sum  F_o $ . $\beta R_w = [\sum [w(F_o^2 - F_c^2)^2] / \sum w(F_o^2)^2]^{1/2}$ .			

## RESULTS AND DISCUSSION

**Description of Crystal Structure.** Single-crystal X-ray diffraction analysis of 1 reveals that it crystallizes in the monoclinic space group C2/c (see Table 1) and has a 3D framework structure. The asymmetric unit of 1 contains two unique formate anions, one Na<sup>+</sup> and half of a Co<sup>2+</sup> ion. The Co1 ion locates in the inversion center with a compressed octahedral coordination configuration, while the Na<sup>+</sup> ion is surrounded by seven oxygen atoms (Figure S3 in the SI). As shown in Figure 1, each Co1 is coordinated by six different formate anions with two kinds of configurations, of which one kind of formate anion links four Na<sup>+</sup> ions and one Co<sup>2+</sup> ion with a bridge-chelate mode and the other kind of formate anion takes a syn,syn,anti,anti mode to link two Na<sup>+</sup> and two Co<sup>2+</sup> ions. All of the Co<sup>2+</sup> ions are linked in the equatorial plane with the second kind of formate to form 2D (4,4) layers (Figure 1b) and the first kind of formate anions take the apical positions of Co<sup>2+</sup> ions. The cobalt(2+) formate layer is anionic for the superfluous coordination of formate anions. The charge is balanced by the Na<sup>+</sup> ions between the layers to form sandwich-like layers (Figure 1c), which are connected by the linkage of Na<sup>+</sup> ions and formate anions on both sides of the layers and finally form a 3D framework (Figure 1d).

2 crystallizes in the cubic space group I2<sub>1</sub>3, and its asymmetric unit contains half of a formate anion, with one-third of the metal position M<sup>1.5+</sup> being occupied by Co<sup>2+</sup> and Na<sup>+</sup> ions together with a 1:1 ratio. The topology structure of 2 is the same as that of the reported manganese formate,<sup>6b</sup> but their crystal structures have some differences. In the manganese formate,<sup>6b</sup> the Mn<sup>2+</sup> and Na<sup>+</sup> ions take two different positions, but in 2, the Co<sup>2+</sup> and Na<sup>+</sup> ions are disordered in one position. The M<sup>1.5+</sup> ion has an octahedral configuration coordinated by six oxygen atoms (Figure 2a). The formate anions bridge four M<sup>1.5+</sup> in a syn,syn,anti,anti mode with the bond angle of M–O–M = 95.77(5)°. In that way, the M<sup>1.5+</sup> ions are connected to 12 neighbors by 6  $\mu_4$  formate anions to form a 3D network, in which the metal ions can be divided into two equal sets of nets linked by the syn,anti formate (Figure 2b). In each set, the

**Table 2. Selected Bond Lengths [Å] and Angles [deg] for 1–3**

Complex 1 <sup>a</sup>			
Co1–O1#1	2.0935(14)	Na1–O4#2	2.3944(14)
Co1–O1	2.0935(14)	Na1–O2#4	2.4134(16)
Co1–O4#2	2.1098(13)	Na1–O2#5	2.4249(16)
Co1–O4#3	2.1098(13)	Na1–O3	2.4429(15)
Co1–O3#1	2.1134(12)	Na1–O2#6	2.5147(17)
Co1–O3	2.1134(12)	Na1–O1#6	2.5778(16)
Na1–O1#1	2.6750(16)		
Complex 2 <sup>b</sup>			
Co1/Na1–O1#4	2.1971 (11)	Co1/Na1–O1#3	2.2490 (13)
Co1/Na1–O1#2	2.1971 (11)	Co1/Na1–O1#1	2.2490 (13)
Co1/Na1–O1	2.1971 (11)	Co1/Na1–O1#5	2.2490 (13)
Co1/Na1–Co1#3/ Na1#3	95.77 (5)		
Complex 3 <sup>c</sup>			
Co1–O9#1	2.065(7)	Co3–O4	2.111(6)
Co1–O9	2.065(7)	Co3–O2	2.141(7)
Co1–O5#1	2.109(6)	Co3–O10	2.143(6)
Co1–O5	2.109(6)	Co3–O5	2.158(7)
Co1–O2#1	2.128(6)	Co4–O8	2.069(7)
Co1–O2	2.128(6)	Co4–O15#4	2.070(6)
Co2–O1	2.070(7)	Co4–O13	2.087(7)
Co2–O15	2.077(7)	Co4–O10	2.123(7)
Co2–O11	2.093(7)	Co4–O12#4	2.120(7)
Co2–O6#2	2.104(7)	Co4–O3#4	2.133(7)
Co2–O3	2.106(7)	Na1–O7#3	2.365(7)
Co2–O14	2.151(7)	Na1–O12#5	2.373(7)
Co3–O7#3	2.074(7)	Na1–O4#3	2.407(8)
Co3–O7	2.074(7)	Na1–O6#3	2.418(7)
Co3–O14	2.112(7)	Na1–O13#6	2.483(8)
Co3–O4#3	2.111(6)	Na1–O11#7	2.513(8)
Co1–O5–Co3	97.7(3)	Co4#8–O15– Co2	100.6(3)
Co4–O10–Co3	114.0(3)	Co2–O3–Co4#8	97.6(3)
Co3–O14–Co2	117.0(3)	Co1–O2–Co3	97.6(3)

<sup>a</sup>Symmetry code: #1,  $-x + 1/2, -y + 1/2, -z + 1$ ; #2,  $-x + 1/2, y + 1/2, -z + 1/2$ ; #3,  $x, -y, z + 1/2$ ; #4,  $x + 1/2, -y + 1/2, z + 1/2$ ; #5,  $-x + 1/2, -y + 1/2, -z$ ; #6,  $-x + 1/2, y - 1/2, -z + 1/2$ . <sup>b</sup>Symmetry code: #1,  $-z, x + 1/2, -y + 1/2$ ; #2,  $y - 1/2, -z + 1/2, -x$ ; #3,  $-x, -y + 1/2, z$ ; #4,  $-z, -x + 1/2, y$ ; #5,  $-y, -z + 1/2$ . <sup>c</sup>Symmetry code: #1,  $-x, -y + 2, -z + 1$ ; #2,  $x + 1, y, z$ ; #3,  $x, y, z$ ; #4,  $x, y + 1, z$ ; #5,  $-x, -y + 1, -z$ ; #6,  $-x, -y + 2, -z$ ; #7,  $x - 1, y, z$ ; #8,  $x, y - 1, z$ .

$M^{1.5+}$  ions are connected to six neighbors with the same  $M \cdots M$  distance of about 5.59 Å (Figure 2c), and the two sets of nets share the same formate anions, forming the final structure of **2** (Figure 2d). From a topological view, in each syn,anti formate bridged net, the  $M^{1.5+}$  ions could be considered as a 6-connected node and both of the two nets could be simplified as a lcy topology net (Figure 3a,b).<sup>6b</sup> Furthermore, both of the two copies of nets have the same chirality. The  $M^{1.5+}$  ions of the lcy nets connect directly to the nearest  $M^{1.5+}$  ions in the other copy of the lcy net by double  $\mu_2$ -oxygen atoms of the formate anions. If neglecting the linkage of the carbon atoms of the formate, a (10,3)-a net would be generated (Figure 3c).<sup>13</sup> However, taking the connections of the formate between the  $M^{1.5+}$  ions into account, **2** could be viewed as a 4,6-connected net with a notation symbol of  $\{4^3;6^2;8\}_3\{4^9;6^6\}_2$  (Figure 3d).<sup>14</sup>

**3** crystallizes in the triclinic space group  $P\bar{1}$ , and the asymmetric unit of **3** contains eight formate anions, one  $Na^+$  ion, and four  $Co^{2+}$  ions in which Co1 locates in the inverse

center, being only half-occupied. Both  $Na^+$  and  $Co^{2+}$  ions in **3** are six-coordinated by the oxygen atoms from formate anions. The  $Co^{2+}$  ions show octahedral configurations, while the  $Na^+$  ions take trigonal-prismatic configurations. The formate anions in **3** could be classified as five different types depending on their coordinated environments. As shown in Figure 4a, the first type containing C1 and C5 takes a syn,syn,anti mode to bridge Co1, Co2, and Co3 or Co1, Co3, and Co4. The second type takes a syn,syn,anti,anti mode to link three  $Co^{2+}$  and one  $Na^+$  ions, in which the formate containing C2 and C7 bridges three  $Co^{2+}$  ions in a syn,syn,anti mode while the formate containing C3 bridges three  $Co^{2+}$  ions in a syn,anti anti mode. The third type of formate anion containing C6 links two  $Co^{2+}$  ions in a syn,syn mode and two  $Na^+$  ions in an anti,anti mode. The fourth type of formate anion containing C4 coordinates to two  $Co^{2+}$  and one  $Na^+$  ions in a syn,syn,anti mode. The last type of formate containing C8 bridges Co2 and Co4 with O15, leaving the other oxygen atom O16 uncoordinated. Then the structure of **3** could be comprehended as follows: the first type of formate anion bridges  $Co^{2+}$  ions to form a 10-membered cobalt ring (Figure 5a), and the rings are interconnected by sharing part of the linkage to form a 1D chain, which is further expanded via the formate anions containing C3 to form a 2D layer (Figure 5b). Finally, a 3D structure is formed by connection of the  $Na^+$  ions between the 2D  $Co^{2+}$  layers (Figure 5c).

In a comparison to other alkali anions like  $K^+$  or ammonium, which take the role of template in a metal formate system,  $Na^+$  has smaller size, which results in shorter  $Co \cdots Co$  distances in order to have the maximum effective packing.<sup>10e</sup> Thus, in **1**, the formate anions adopt a syn,anti mode to link  $Co^{2+}$  ions, not like in the nicolite-,<sup>5f,8f</sup> perovskite-,<sup>3b,5e</sup> and chiral-related<sup>4f,10e</sup> metal formates templated by big cations in which the formate takes an anti,anti mode. In **2** and **3**, there are less  $Na^+$  ions in the structure; thus, the syn,syn,anti,anti, syn,anti,anti, and syn,syn,anti formate anions present link  $Co^{2+}$  ions with more small  $Co \cdots Co$  distances.

**Magnetic Studies.** Magnetic measurements were carried out on well-crushed crystalline samples of **1–3** (phase purity of the samples confirmed by PXRD; see Figure S4 in the SI), and different magnetic behaviors were found to exist in the three complexes.

The magnetic properties of **1** are shown in Figure 6 as  $\chi_m T$  vs  $T$  and  $M/N\mu_B$  vs  $H$  plots, assuming a crystallographic unit containing one  $Co^{2+}$  ion for the molar weight. The  $\chi_m T$  values first increase smoothly up to 3.62  $cm^3 K mol^{-1}$  from room temperature to 130 K, and then the value decreases to a minimum value of 3.14  $cm^3 K mol^{-1}$  at 15 K before increasing quickly. The best-fit parameters from the magnetic data recorded at 100–300 K through the Curie–Weiss law (Figure S5 in the SI) are  $\theta = 7.43$  K and  $C = 3.43 cm^3 K mol^{-1}$ . The Weiss constant for one magnetically isolated high-spin  $Co^{2+}$  ion with spin–orbit coupling is about  $-20$  K.<sup>15</sup> Thus, the positive Weiss constant of **1** suggests ferromagnetic coupling between adjacent  $Co^{2+}$  ions in the layer structure of **1**. The minimum of the  $\chi_m T$  vs  $T$  plots is due to the cooperative effects of the ferromagnetic interactions between  $Co^{2+}$  ions and spin–orbit coupling of the single  $Co^{2+}$  ion.<sup>16</sup> The syn,anti formate should be expected to mediate weak ferromagnetic interactions between  $Co^{2+}$  ions.<sup>17,18</sup> Also, the field-dependent magnetizations at 2 K (Figure 6, inset) clearly corroborate the ferromagnetic coupling between  $Co^{2+}$  ions. On the other hand, the  $M/N\mu_B$  curve does not follow the Brillouin function. With an increase of the field, it reaches a saturation value quickly at

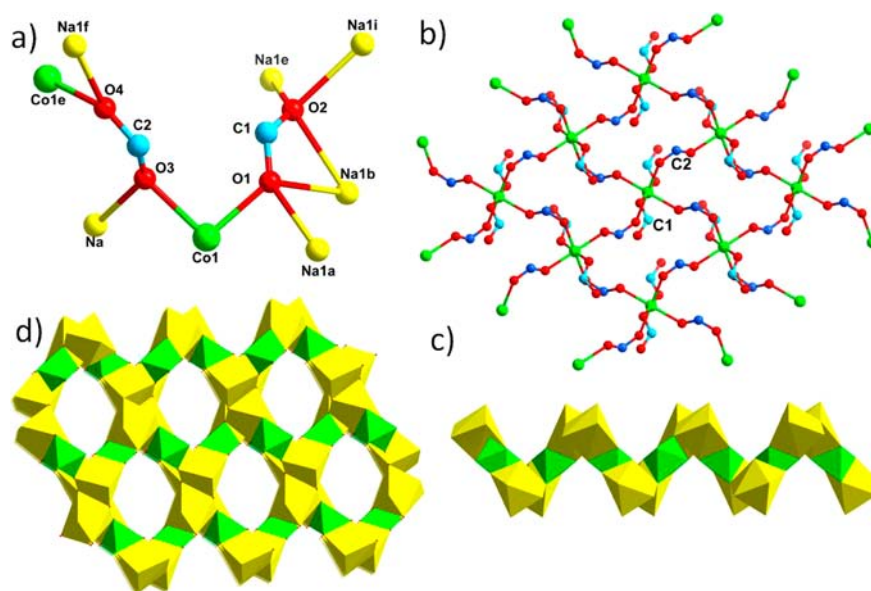


**Figure 1.** (a) Linkage mode of the formate anions in **1**. (b) 2D cobalt formate layer in **1**. (c) Polyhedral view of the sandwich-like NaCoNa layer in **1**. (d) Polyhedral view of the 3D structure of **1**.

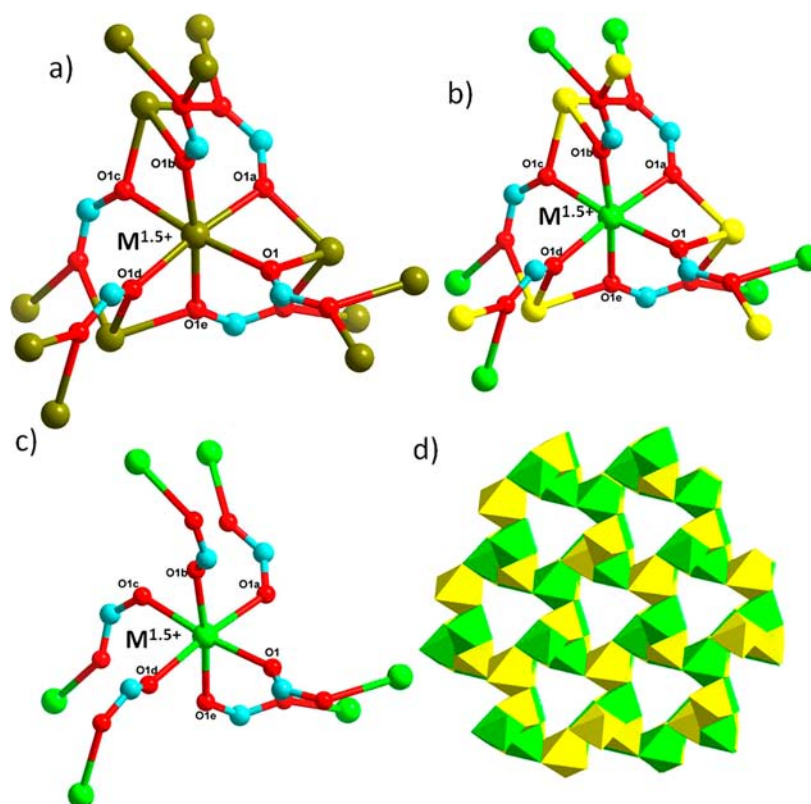


**Figure 2.** (a) Linkage mode of  $M^{1.5+}$  ions in **2**. (b) Linkage mode of the two copies of  $M^{1.5+}$  ions by a syn,anti formate in **2**. (c) Coordination mode of the  $M^{1.5+}$  in each copy of syn,anti formate linked nets in **2**. (d) Polyhedral view of the 3D structure of **2**.

about 1 T, and the  $M/N\mu_B$  value at 5 T is close to  $3.3N\mu_B$ . The zero-field-cooled and field-cooled magnetization curves under 100 Oe are completely identical, excluding the long-range ferromagnetic order in the ferromagnetic layers being well separated by the  $Na^+$  ions (Figure S6 in the SI).

The magnetic properties of **2** are shown in Figure 7 as  $\chi_m T$  vs  $T$  and  $M/N\mu_B$  vs  $H$  plots, assuming a crystallographic unit containing one  $Co^{2+}$  ion for the molar weight. The  $\chi_m T$  curve

starts to decrease from room temperature upon cooling and reaches  $0.81 \text{ cm}^3 \text{ K mol}^{-1}$  at 2 K. The best-fit parameters from the magnetic data in the temperature range 50–300 K through the Curie–Weiss law (Figure S5 in the SI) are  $\theta = -23.75 \text{ K}$  and  $C = 3.49 \text{ cm}^3 \text{ K mol}^{-1}$ . The Weiss constant is less than  $-20 \text{ K}$ , indicating antiferromagnetic interactions conducted by the syn, syn,anti,anti formate anions between  $Co^{2+}$  ions.<sup>15</sup> The field-dependent magnetizations at 2 K (Figure 7, inset)

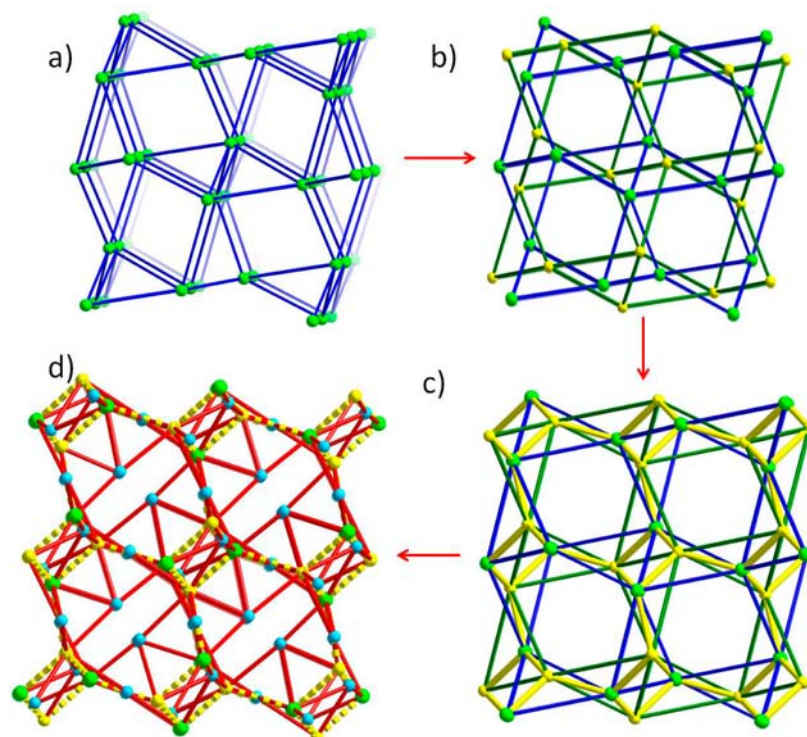


**Figure 3.** (a) lcy topology nets of  $M^{1.5+}$  linked by syn,anti formate in **2**. (b) Two lcy nets formed by the two copies of syn,anti formate and  $M^{1.5+}$  ions in **2**. (c) (10,3)-a net formed by the  $M^{1.5+}$  ion in two copies of lcy nets. (d) 4,6-Connected net formed by the  $M^{1.5+}$  ( $Co^{2+}$  and  $Na^+$ ) ions and formate anions.

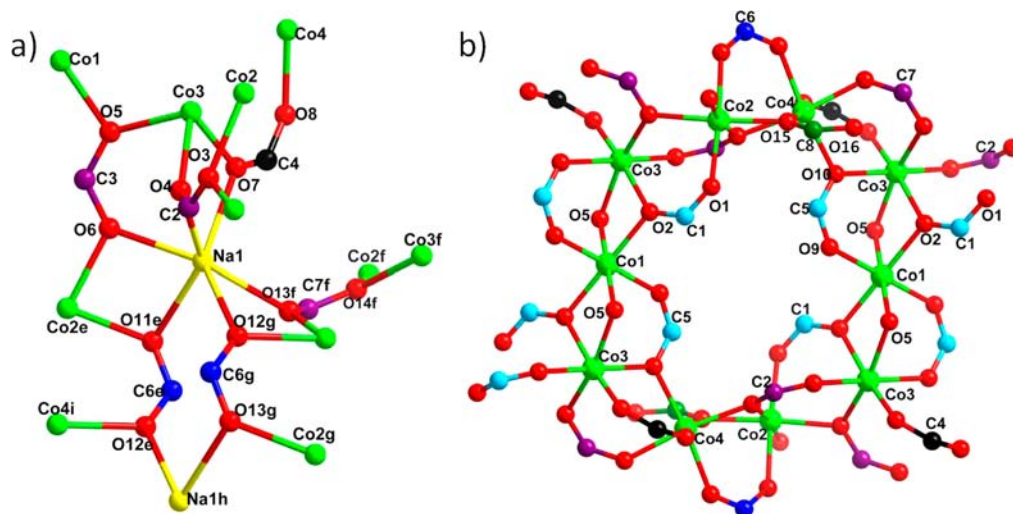


**Figure 4.** (a) Coordination mode of the  $Na^+$  ions and some formate anions in **3**. (b) 10-membered  $Co^{2+}$  ring in **3**.

corroborate the antiferromagnetic coupling because the curve shows an increasing trend along with an increase of the field almost linearly without saturation.<sup>15</sup>

For **3**, the  $\chi_m T$  vs  $T$  and  $M/N\mu_B$  vs  $H$ , assuming one  $Co^{2+}$  ion for the molar weight are shown in Figure 8. Starting from room temperature, the  $\chi_m T$  values smoothly decrease until about 10 K, and then it shows a small rise before finally dropping. The best-fit parameters from the magnetic data from 50 to 300 K through the Curie–Weiss law (Figure S5 in the SI) are  $\theta = -25.88$  K and  $C = 3.73$  cm<sup>3</sup> K mol<sup>-1</sup>. Different from that of **1** and **2**, the  $\chi_m$  vs  $T$  plots of **3** show a peak at about 2.5 K, suggesting an antiferromagnetic order in **3** below 2.5 K (Figure S7 in the SI). The increase in  $\chi_m$  with a decrease of the external

field and the  $\chi_m T$  vs  $T$  plots at low temperature may be due to slight impurities in the samples. The field-dependent magnetizations at 2 K (Figure 8, inset) corroborate the antiferromagnetic interactions at low temperature, which has a value of  $2.04 N\mu_B$  at 5 T without saturation. It is worth noting that there is an inflection in the  $M$  vs  $H$  plots. The inflection is obvious, and the first derivative shows a clear maximum at ca. 4000 Oe, indicating that above that field **3** underwent a spin-flop transition from an antiferromagnetic phase to a paramagnetic phase.

In **1–3**, the  $Co^{2+}$  ions linked by the formates in five different modes (Table 3), in which the syn,syn,anti,anti/syn,anti,anti, and syn,syn,anti modes could be viewed as a combination of

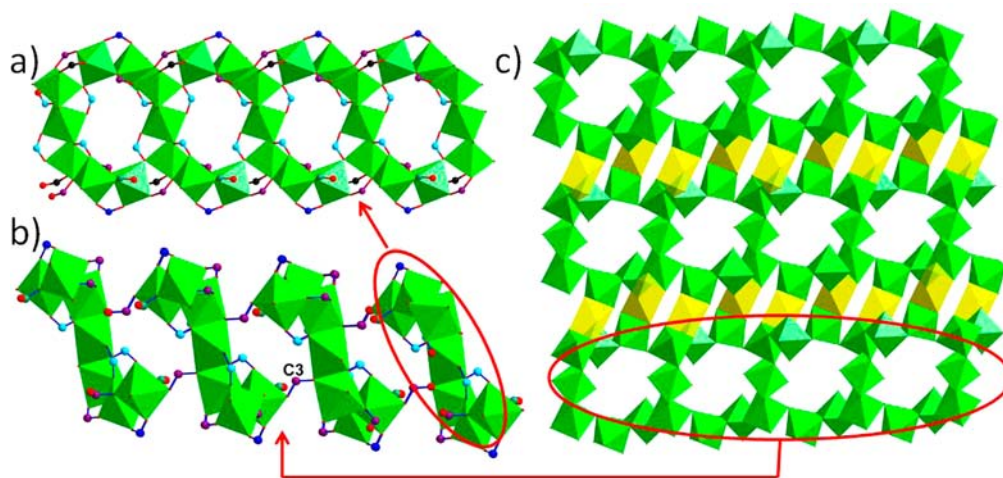


**Figure 5.** (a) 1D chain formed by the 10-membered  $\text{Co}^{2+}$  ring in **3**. (b) Side view of the 2D layer formed by the 1D chains in **3**. (c) Polyhedral view of the 3D structure of **3**.

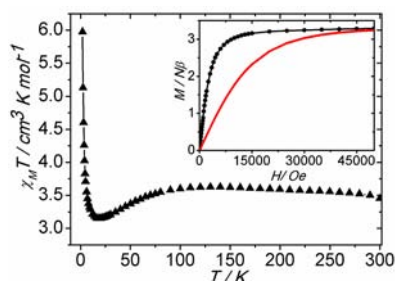


**Figure 6.**  $\chi_m T$  vs  $T$  plots at 0.2 T of **1**. Inset:  $M/N\mu_B$  vs  $H$  plots of **1** at 2 K with a Brillouin function of  $g = 2.2$  and  $S = 3/2$  (red line).

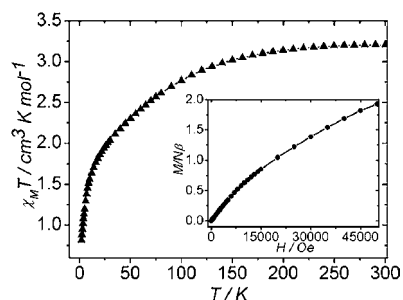


**Figure 7.**  $\chi_m T$  vs  $T$  plots at 0.2 T of **2**. Inset:  $M/N\mu_B$  vs  $H$  plots of **2** at 2 K.

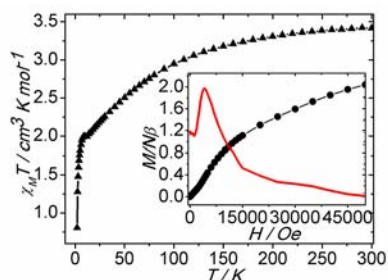


**Figure 8.**  $\chi_m T$  vs  $T$  plots at 0.1 T of **3**. Inset: Sigmoidal shape of  $M/N\mu_B$  vs  $H$  plots of **3** at 2 K together with its first derivative (red line).

four basic modes: syn,syn, anti,anti, syn,anti, and  $\mu_2$ -O modes, which conduct magnetic coupling, respectively. The syn,syn mode conducts strong antiferromagnetic interactions between

**Table 3.** Magnetic Behaviors Conducted by Different Coordinated Carboxylates between  $\text{Co}^{2+}$  Ions in **1–3**

complex	coordination mode	magnetic exchange	ref <sup>a</sup>
<b>1</b>	syn,anti	F	17
<b>2</b>	syn,syn,anti,anti	syn,anti	3c, 5e, 6f, 7e
		anti,anti	3b, 3e, 4a, 6f, 6g
		syn,syn	3c, 5e, 6f, 7e
		$\mu_2$ -O	3c, 5e, 6f, 7e
<b>3</b>	syn,syn	AF	3c, 5e, 6f, 7e
	syn,anti,anti	syn,anti	3c, 5e, 6f, 7e
		anti,anti	3b, 3e, 4a, 6f, 6g
		$\mu_2$ -O	3c, 5e, 6f, 7e
	syn,syn,anti	syn,syn	3c, 5e, 6f, 7e
		syn,anti	3c, 5e, 6f, 7e
		$\mu_2$ -O	3c, 5e, 6f, 7e
	$\mu_2$ -O	AF	3c, 5e, 6f, 7e

<sup>a</sup>Ligands in ref 17 are carboxylates; ref 3c contains syn,syn,anti formates; ref 5e contains syn,syn,anti formates; ref 6f contains three types of formates in syn,anti/anti,anti/syn,anti,anti; ref 7e contains syn,syn,anti,anti formates.

adjacent  $\text{Co}^{2+}$  ions, while the anti,anti, and syn,anti modes mediate weak ferromagnetic or antiferromagnetic coupling,<sup>4</sup> and the magnetic interactions conducted by the  $\mu_2$ -O mode depend on the Co–O–Co angle with a critical value of  $90^\circ$ . The antiferromagnetic interactions conducted by formate in the four basic modes are familiar. Thus, the antiferromagnetism of **2** and **3** is common, while the ferromagnetic interaction in **1** is infrequent but not surprising in formate or carboxylate complexes.<sup>17</sup> The magnetic interactions conducted by different carboxylates between adjacent  $\text{Co}^{2+}$  ions in **1–3** and some reported complexes have been summarized in Table 3.

## CONCLUSION

Three new heterometallic formate coordination polymers formulated as  $[\text{Na}_2\text{Co}(\text{HCOO})_4]_\infty$  (**1**),  $[\text{NaCo}(\text{HCOO})_3]_\infty$  (**2**), and  $[\text{Na}_2\text{Co}_7(\text{HCOO})_{16}]_\infty$  (**3**) have been obtained by adjusting the solvent and ratio of the reactants. The ferromagnetic interactions exist between adjacent  $\text{Co}^{2+}$  ions in **1**, while dominating antiferromagnetic couplings in **2** and **3** were found.

## ■ ASSOCIATED CONTENT

## ● Supporting Information

X-ray crystallographic data in CIF format for 1–3 and Figures S1–S7. This material is available free of charge via the Internet at <http://pubs.acs.org>.

## ■ AUTHOR INFORMATION

## Corresponding Author

\*E-mail: [buxh@nankai.edu.cn](mailto:buxh@nankai.edu.cn). Fax: +86-22-23502458. Tel: +86-22-23502809.

## Notes

The authors declare no competing financial interest.

## ■ ACKNOWLEDGMENTS

This work was supported by the NNSF of China (Grants 21031002 and 21101114), the 973 Program of China (Grant 2012CB821700), and the Natural Science Fund of Tianjin, China (Grant 10JCZDJC22100).

## ■ REFERENCES

- (1) For examples, see: (a) Thomas, L.; Lionti, F.; Ballou, R.; Gatteschi, D.; Sessoli, R.; Barbara, B. *Nature* **1996**, *383*, 145. (b) Turnbull, M. M.; Sugimoto, T.; Thompson, L. K. *Molecule-Based Magnetic Materials*; American Chemical Society: Washington, DC, 1996. (c) Gatteschi, D.; Sessoli, R. *Angew. Chem., Int. Ed.* **2003**, *43*, 268. (d) Liu, T.-F.; Fu, D.; Gao, S.; Zhang, Y.-Z.; Sun, H.-L.; Su, G.; Liu, Y.-J. *J. Am. Chem. Soc.* **2003**, *125*, 13976. (e) Wang, S.; Zuo, J.-L.; Gao, S.; Zhou, H.-C.; Zhang, Y.-Z.; You, X.-Z. *J. Am. Chem. Soc.* **2004**, *126*, 8900. (f) Gatteschi, D.; Sessoli, R.; Villain, J. *Molecular Nanomagnets*; Oxford University Press: Oxford, U.K., 2006.
- (2) For examples, see: (a) Coronado, E.; Galán-Mascarós, J. R.; Martí-Gastaldo, C. *J. Am. Chem. Soc.* **2008**, *130*, 14987. (b) Rood, J. A.; Noll, B. C.; Henderson, K. W. *Inorg. Chem.* **2006**, *45*, 5521. (c) Liu, T.; Zhang, Y.-J.; Wang, Z.-M.; Gao, S. *J. Am. Chem. Soc.* **2008**, *130*, 10500. (d) Zheng, Y.-Z.; Tong, M.-L.; Zhang, W.-X.; Chen, X.-M. *Angew. Chem., Int. Ed.* **2006**, *45*, 6310. (e) Wang, X.-Y.; Wang, Z.-M.; Gao, S. *Chem. Commun.* **2008**, 281.
- (3) (a) Dybtsev, D. N.; Chun, H.; Yoon, S. H.; Kim, D.; Kim, K. *J. Am. Chem. Soc.* **2004**, *126*, 32. (b) Wang, X.-Y.; Gan, L.; Zhang, S.-W.; Gao, S. *Inorg. Chem.* **2004**, *43*, 4615. (c) Wang, Z.; Zhang, B.; Kurmoo, M.; Green, M. A.; Fujiwara, H.; Otsuka, T.; Kobayashi, H. *Inorg. Chem.* **2005**, *44*, 1230. (d) Wang, Z.; Zhang, B.; Otsuka, T.; Inoue, K.; Kobayashi, H.; Kurmoo, M. *Dalton Trans.* **2004**, 2209. (e) Rettig, S. J.; Thompson, R. C.; Trotter, J.; Xia, S. *Inorg. Chem.* **1999**, *38*, 1360. (f) Wang, Z.-M.; Hu, K.-L.; Gao, S.; Kobayashi, H. *Adv. Mater.* **2010**, *22*, 1526 and references cited therein.
- (4) (a) Calderone, P. J.; Forster, P. M.; Borkowski, L. A.; Teat, S. J.; Feyngenson, M.; Aronson, M. C.; Parise, J. B. *Inorg. Chem.* **2011**, *50*, 2159. (b) Manson, J. L.; Lancaster, T.; Schlueter, J. A.; Blundell, S. J.; Brooks, M. L.; Pratt, F. L.; Nygren, C. L.; Koo, H. J.; Dai, D.; Whangbo, M. H. *Inorg. Chem.* **2007**, *46*, 213. (c) Manson, J. L.; Lecher, J. G.; Gu, J.; Geiser, U.; Schlueter, J. A.; Henning, R.; Wang, X.; Schultz, A. J.; Koo, H.-J.; Whangbo, M.-H. *Dalton Trans.* **2003**, 2905. (d) Sapina, F.; Burgos, M.; Escriba, E.; Folgado, J. V.; Marcos, D.; Beltran, A.; Beltran, D. *Inorg. Chem.* **1993**, *32*, 4337. (e) Hu, B.-W.; Zhao, J.-P.; Yang, Q.; Zhang, X.-F.; Bu, X.-H. *Sci. China, Ser. B* **2009**, *52*, 1451. (f) Xu, G.-C.; Zhang, W.; Ma, X.-M.; Cheng, Y.-H.; Zhang, L.; Cai, H.-L.; Wang, Z.-M.; Xiong, R.-G.; Gao, S. *J. Am. Chem. Soc.* **2011**, *133*, 14948. (g) Xu, G.-C.; Ma, X.-M.; Zhang, L.; Wang, Z.-M.; Gao, S. *J. Am. Chem. Soc.* **2010**, *132*, 9588.
- (5) (a) Fang, Q.-R.; Zhu, G.-S.; Jin, Z.; Xue, M.; Wei, X.; Wang, D.-J.; Qiu, S.-L. *Angew. Chem., Int. Ed.* **2006**, *45*, 6126. (b) Zhang, J.; Chen, S.; Valle, H.; Wong, M.; Austria, C.; Cruz, M.; Bu, X. *J. Am. Chem. Soc.* **2007**, *129*, 14168. (c) Zhang, Z.-M.; Yao, S.; Li, Y.-G.; Clérac, R.; Lu, Y.; Su, Z.-M.; Wang, E.-B. *J. Am. Chem. Soc.* **2009**, *131*, 14600. (d) Zhao, J.-P.; Hu, B.-W.; Yang, Q.; Hu, T.-L.; Bu, X.-H. *Inorg. Chem.* **2009**, *48*, 7111. (e) Shang, R.; Sun, X.; Wang, Z.-M.; Gao, S. *Chem.—Asian J.* **2012**, *7*, 1697. (f) Li, M.-Y.; Kurmoo, M.; Wang, Z.-M.; Gao, S. *Chem.—Asian J.* **2011**, *6*, 3084. (g) Liu, B.; Shang, R.; Hu, K.-L.; Wang, Z.-M.; Gao, S. *Inorg. Chem.* **2012**, *51*, 13363.
- (6) (a) Viertelhaus, M.; Adler, P.; Clérac, R.; Anson, C. E.; Powell, A. K. *Eur. J. Inorg. Chem.* **2005**, 692. (b) Paredes-García, V. N.; Vega, A. S.; Novak, M. A.; Vaz, M. G. F.; Souza, D. A.; Venegas-Yazigi, D.; Spodine, E. *Inorg. Chem.* **2009**, *48*, 4737. (c) Rodriguez-Dieguez, A.; Kivekas, R.; Sakiyama, H.; Debdoubi, A.; Colacio, E. *Dalton Trans.* **2007**, 2145. (d) Manson, J. L.; Lancaster, T.; Chapon, L. C.; Blundell, S. J.; Schlueter, J. A.; Brooks, M. L.; Pratt, F. L.; Nygren, C. L.; Qualls, J. S. *Inorg. Chem.* **2005**, *44*, 989. (e) Kageyama, H.; Khomskii, D. I.; Levitin, R. Z.; Vasil'ev, A. N. *Phys. Rev. B* **2003**, *67*, 224422. (f) Li, Z.-X.; Zhao, J.-P.; Sañudo, E. C.; Ma, H.; Pan, Z.-D.; Zeng, Y.-F.; Bu, X.-H. *Inorg. Chem.* **2009**, *48*, 11601. (g) Wang, X.-Y.; Wei, H.-Y.; Wang, Z.-M.; Chen, Z.-D.; Gao, S. *Inorg. Chem.* **2005**, *44*, 572.
- (7) (a) Alborès, P.; Rentschler, E. *Angew. Chem., Int. Ed.* **2009**, *48*, 9366. (b) Bi, Y.; Wang, X.-T.; Liao, W.; Wang, X.; Zhang, H.; Gao, S. *J. Am. Chem. Soc.* **2009**, *131*, 11650. (c) Bi, Y.; Xu, G.; Liao, W.; Du, S.; Wang, X.; Deng, R.; Zhang, H.; Gao, S. *Chem. Commun.* **2010**, 6362. (d) Lisnard, L.; Tuna, F.; Candini, A.; Affronte, M.; Wimpenny, R. E. P.; McInnes, E. J. L. *Angew. Chem., Int. Ed.* **2008**, *47*, 9695. (e) Zhao, J.-P.; Yang, Q.; Zhong, Y.-L.; Zhao, Z.; Du, M.; Chang, Z.; Bu, X.-H. *Chem. Commun.* **2012**, *48*, 6568.
- (8) For examples, see: (a) Costes, J.-P.; Dahan, F.; García-Tojal, J. *Chem.—Eur. J.* **2002**, *8*, 5430. (b) Gavrilenko, K. S.; Punin, S. V.; Cador, O.; Golhen, S.; Ouahab, L.; Pavlishchuk, V. V. *J. Am. Chem. Soc.* **2005**, *127*, 12246. (c) Noro, S.-i.; Miyasaka, H.; Kitagawa, S.; Wada, T.; Okubo, T.; Yamashita, M.; Mitani, T. *Inorg. Chem.* **2004**, *44*, 133. (d) Pardo, E.; Cangussu, D.; Dul, M.-C.; Lescouëzec, R.; Herson, P.; Journaux, Y.; Pedroso, E. F.; Pereira, C. L. M.; Muñoz, M. C.; Ruiz-García, R.; Cano, J.; Amorós, P.; Julve, M.; Lloret, F. *Angew. Chem., Int. Ed.* **2008**, *47*, 4211. (e) Peng, J.-B.; Zhang, Q.-C.; Kong, X.-J.; Zheng, Y.-Z.; Ren, Y.-P.; Long, L.-S.; Huang, R.-B.; Zheng, L.-S.; Zheng, Z. *J. Am. Chem. Soc.* **2012**, *134*, 3314. (f) Zhao, J.-P.; Hu, B.-W.; Lloret, F.; Tao, J.; Yang, Q.; Zhang, X.-F.; Bu, X.-H. *Inorg. Chem.* **2010**, *49*, 10390.
- (9) (a) Cheng, X. N.; Zhang, W. X.; Lin, Y. Y.; Zheng, Y. Z.; Chen, X. M. *Adv. Mater.* **2007**, *19*, 1494. (b) Dul, M.-C.; Pardo, E.; Lescouëzec, R.; Chamoiseau, L.-M.; Villain, F.; Journaux, Y.; Ruiz-García, R.; Cano, J.; Julve, M.; Lloret, F.; Pasán, J.; Ruiz-Pérez, C. *J. Am. Chem. Soc.* **2009**, *131*, 14614. (c) Duran, N.; Clegg, W.; Cucurull-Sánchez, L.; Coxall, R. A.; Jiménez, H. R.; Moratal, J.-M.; Lloret, F.; González-Duarte, P. *Inorg. Chem.* **2000**, *39*, 4821. (d) Hursthouse, M. B.; Light, M. E.; Price, D. J. *Angew. Chem., Int. Ed.* **2004**, *43*, 472. (e) Li, Y.; Xiang, S.; Sheng, T.; Zhang, J.; Hu, S.; Fu, R.; Huang, X.; Wu, X. *Inorg. Chem.* **2006**, *45*, 6577. (f) Murrie, M.; Teat, S. J.; Stoeckli-Evans, H.; Güdel, H. U. *Angew. Chem., Int. Ed.* **2003**, *42*, 4653. (g) Xiang, S.-C.; Wu, X.-T.; Zhang, J.-J.; Fu, R.-B.; Hu, S.-M.; Zhang, X.-D. *J. Am. Chem. Soc.* **2005**, *127*, 16352.
- (10) (a) Zheng, Y.-Q.; Lin, J.-L.; Xu, W.; Xie, H.-Z.; Sun, J.; Wang, X.-W. *Inorg. Chem.* **2008**, *47*, 10280. (b) Yang, H.; Chen, J.-M.; Sun, J.-J.; Yang, S.-P.; Yu, J.; Tan, H.; Li, W. *Dalton Trans.* **2009**, 2540. (c) Wang, C.-F.; Gao, E.-Q.; He, Z.; Yan, C.-H. *Chem. Commun.* **2004**, 720. (d) Galloway, K. W.; Schmidtman, M.; Sanchez-Benitez, J.; Kamenev, K. V.; Wernsdorfer, W.; Murrie, M. *Dalton Trans.* **2010**, 4727. (e) Duan, Z.; Wang, Z.; Gao, S. *Dalton Trans.* **2011**, 4465. (f) Chen, Z.; Li, Y.; Jiang, C.; Liang, F.; Song, Y. *Dalton Trans.* **2009**, 5290.
- (11) Liu, F.-C.; Ouyang, J. *Acta Crystallogr., Sect. E* **2007**, m2557.
- (12) (a) *CrystalClear and CrystalStructure*; Rigaku/MS: The Woodlands, TX, 2005. (b) Sheldrick, G. M. *SHELXTL NT: Program for Solution and Refinement of Crystal Structures*, version 5.1; University of Göttingen: Göttingen, Germany, 1997.
- (13) Hu, B.-W.; Zhao, J.-P.; Yang, Q.; Liu, F.-C.; Bu, X.-H. *J. Mater. Chem.* **2009**, *19*, 6827.
- (14) (a) Reticular Chemistry Structure Resource (RCSR), <http://rcsr.anu.edu.au>. (b) Euclidean Patterns in Non-Euclidean Tilings

(EPINET), <http://epinet.anu.edu.au>. (c) Blatov, V. A.; Shevchenko, A. P. *TOPOS 4.0*; Samara State University, Samara, Russia, 2003.

(15) (a) Kurmoo, M. *Chem. Soc. Rev.* **2009**, *38*, 1353. (b) Mabbs, F. E.; Machin, D. J. *Magnetism and Transition Metal Complexes*; Chapman and Hall: London, 1973. (c) Lines, M. E. J. *Chem. Phys.* **1971**, *55*, 2977.

(16) Lloret, F.; Julve, M.; Cano, J.; Ruiz-García, R.; Pardo, E. *Inorg. Chim. Acta* **2008**, *361*, 3432.

(17) For examples, see: (a) Nadeem, M. A.; Bhadbhade, M.; Bircher, R.; Stride, J. A. *Cryst. Growth Des.* **2010**, *10*, 4060. (b) Chu, Q.; Su, Z.; Fan, J.; Okamura, T.; Lv, G.-C.; Liu, G.-X.; Sun, W.-Y.; Ueyama, N. *Cryst. Growth Des.* **2011**, *11*, 3885. (c) Wang, S.; Bai, J.; Xing, H.; Li, Y.; Song, Y.; Pan, Y.; Scheer, M.; You, X.-Z. *Cryst. Growth Des.* **2007**, *4*, 747.

(18) Jia, H.-P.; Li, W.; Ju, Z.-F.; Zhang, J. *Chem. Commun.* **2008**, 371.